出國報告(出國類別：出席國際研討會發表論文)

出席 2009 年 IEEE 自動化科學與工程國際研討會報告

服務機關：國防大學理工學院電機電子工程學系
姓名職稱：洪敏雄 教授
派赴國家：印度
報告日期：98 年 9 月 30 日
出國時間：98 年 8 月 21 日至 98 年 8 月 22 日

摘要

本次出國之目的爲參加98年8月22日至25日在於印度班加羅爾市(Bangalore, India)舉行之2009 年IEEE自動化科學與工程國際研討會(2009 IEEE International Conference on Automation Science and Engineering, CASE 2009)，並發表學術研究論文。本次CASE 2009國際研討會共有214篇論文投稿，審查結果僅118篇論文獲接受於本次大會發表，接受率僅約55%。本次大會於98年8月22日於印度科學院(Indian Institute of Science)舉行4場Workshops與4場Tutorials，本人也報名參加了Tutorial: Sensor Networks for Automation Applications及Workshop: Service Science and Automation，學習不少相關技術與知識。本次大會共舉辦了三場全體出席的大會演講(Plenary Talks)，分別由兩位知名學者:美國康乃狄克大學的Peter Luh教授與美國華盛頓大學Karl Bohringer教授，以及知名軟體公司Infosys Technologies的執行長S. Gopalakrishnan先生擔任講座。本次大會也利用98年8月23日至25日3天時間，分5個平行場次(Parallel Tracks)，共有25場次(Sessions)-包含9個特別場次(Special Sections)，將所有論文利用口頭方式公開發表。本人在本次會議發表論文乙篇「雙重虛擬量測輸出選擇機制之進階研究(Advanced Studies of Selection Schemes for Dual Virtual-Metrology Outputs)」，被安排於98年8月24日下午4點半導體良率症狀辨識自動化(Automation for Yield Symptom Identification in Semiconductor Manufacturing)特別場次報告。

目次

一、目的

本次出國之目的為參加98年8月22日至25日在於印度班加羅爾市(Bangalore, India)舉行之2009 年IEEE自動化科學與工程國際研討會(2009 IEEE International Conference on Automation Science and Engineering, CASE 2009)，並發表學術論文乙篇，經費來源為行政院國家科學委員會補助國內專家學者出席國際學術會議經費。

二、過程

本次2009年IEEE自動化科學與工程國際研討會(CASE 2009)於98年8月22日至25日在印度班加羅爾市(Bangalore, India)舉行。本次會議共有214篇論文投稿，審查結果僅118篇論文獲接受於本次大會發表，接受率僅約55%。

本次大會於98年8月22日於印度科學院(Indian Institute of Science)舉行4場Workshops與4場Tutorials，本人也報名參加了Tutorial: <u>Sensor Networks for Automation Applications</u>及Workshop: <u>Service Science and Automation</u>，學習不少相關技術與知識。本次大會共舉辦了三場全體出席的大會演講(Plenary Talks)，分別由兩位知名學者:美國康乃狄克大學的Peter Luh教授與美國華盛頓大學Karl Bohringer教授，以及知名軟體公司Infosys Technologies的執行長S. Gopalakrishnan先生擔任講座。

本次大會也利用98年8月23日至25日3天時間，分5個平行場次(Parallel Tracks)，共有25場次(Sessions)-包含9個特別場次(Special Sections)，將所有論文利用口頭方式公開發表。本人在本次會議發表論文乙篇「雙重虛擬量測輸出選擇機制之進階研究(Advanced Studies of Selection Schemes for Dual Virtual-Metrology Outputs)」，被安排於98年8月24

日下午4點半導體良率症狀辨識自動化(Automation for Yield Symptom Identification in Semiconductor Manufacturing)特別場次報告，論文資料如下：

(中文題目：雙重虛擬量測輸出選擇機制之進階研究)

Wei-Ming Wu, Fan-Tien Cheng, Tung-Ho Lin, Deng-Lin Zeng, Jyun-Fang Chen, and Min-Hsiung Hung, "Advanced Studies of Selection Schemes for Dual Virtual-Metrology Outputs," in *Proceedings of 2009 IEEE International Conference on Automation Science and Engineering (CASE 2009)*, Bangalore, India, pp. 421-426, August 22-25, 2009.

三、心得

本次大會之特色除了 3 場邀請之專題演講(Invited Plenary Talks)及 4 場 Workshops 與 4 場 Tutorials 外，也舉辦參觀印度軟體公司的參訪活動，讓參與者可以看到印度軟體發展的進步情形。本次國際學術會議，國內共有 6 位的專家學者參加。整體而言，本次大會相當成功。本次研討會從研討會訊息、論文投稿、論文審稿、論文審查意見通知、論文定稿、到研討會註冊報名等均可由 CASE 2009 網站作業完成，資訊非常透明與便捷，此點值得國內辦理研討會時參考。

四、建議事項

最後，感謝國科會提供經費補助國內專家學者出席國際研討會，也期盼國內學者能繼續積極參與國際學術活動並發表論文，以期提升我國之國際學術地位。

五、攜回資料名稱及內容

1. Proceedings CD of 2009 IEEE International Conference on Automation Science and Engineering.

附錄：「雙重虛擬量測輸出選擇機制之進階研究(Advanced Studies of Selection Schemes for Dual Virtual-Metrology Outputs)」論文內容

5th Annual IEEE Conference on Automation Science and Engineering
Bangalore, India, August 22-25, 2009

Advanced Studies of Selection Schemes for Dual Virtual-Metrology Outputs

Wei-Ming Wu, *Student Member, IEEE*, Fan-Tien Cheng*, Fellow, IEEE*, Tung-Ho Lin, *Member, IEEE*, Deng-Lin Zeng, Jyun-Fang Chen, and Min-Hsiung Hung, *Senior Member, IEEE*

Abstract **-- Advanced Studies of selection schemes between neural-network (NN) and multiple-regression (MR) outputs of a virtual metrology system (VMS) are presented in this paper. Both NN and MR are applicable algorithms for implementing VM conjecture models. But a MR algorithm may achieve better accuracy only with a stable process, whereas a NN algorithm may has superior accuracy when equipment property drift or shift occurs. To take advantage of the merits of both MR and NN algorithms, the simple-selection scheme (SS-scheme) was proposed in CASE 2008 to enhance virtual-metrology (VM) conjecture accuracy. This SS-scheme simply selects either NN or MR output. Recently, with advanced studies, a weighted-selection scheme (WS-scheme), which computes the VM output with a weighted sum of NN and MR results, has been developed. Besides the example with the CVD process of fifth generation TFT-LCD used in the CASE 2008 paper, a new example with the photo process is also adopted in this paper to test and compare the conjecture accuracy among solo NN, solo MR, SS-scheme, and WS-scheme. One-hidden-layered back-propagation neural network (BPNN-I) is adopted for establishing the NN conjecture model. Test results show that the conjecture accuracy of the WS-scheme is the best among those of solo NN, solo MR, SS-scheme, and WS-scheme algorithms.**

Index Terms **– Virtual metrology (VM), dual-VM outputs, simple selection scheme (SS-scheme), weighted selection scheme (WS-scheme).**

I. INTRODUCTION

As the size of electronic devices shrink gradually, wafer-to-wafer (W2W) control has become more essential for critical stages in improving semiconductor manufacturing yield rate [1], [2]. To achieve the requirement of W2W control, the metrology values of each wafer needs to be obtained. However, it is very expensive and time-consuming to acquire the metrology values of each wafer by actual measurement. A feasible solution is to apply virtual metrology (VM) technology, which can conjecture the processing quality of each wafer according to the process data of a production tool without physically conducting actual measurement [2]-[4].

Khan *et al*. published twin papers in November 2007 [5] and 2008 [6] to develop a distributed VM architecture for fab-wide VM and feedback control of semiconductor manufacturing processes using recursive partial least squares (PLS). Both [5] and [6] stated that the VM conjecture accuracy will affect the controlled process outputs. Besides, Wu *et al*. [7] studied the performance of run-to-run (R2R) control subject to metrology delay and concluded that applying VM to remedy the metrology-delay problem is justified if the error of the VM method is less than the error caused by stochastic process noise. In other words, with accurate and prompt VM outputs, W2W control can be economically achieved in current semiconductor manufacturing processes. Therefore, to implement VM for supporting R2R/W2W control, high conjecture accuracy is the key issue.

To achieve high VM conjecture accuracy, adopting feature/variable selection methods to filter out noise of process data are possible approaches. Ko *et al*. [8] proposed the so-called autokey method to choose key parameters of VM from the manufacturing data via a hierarchical clustering approach and according to their correlation coefficients. Also, Lin *et al*. [9] developed a NN-based key-variable selection method for enhancing VM accuracy. On the other hands, this paper proposes selection schemes of dual VM outputs to improve VM conjecture accuracy.

As VM is practically applied, no actual metrology value can be used to evaluate conjecture accuracy. Thus, the VM conjecture value needs an accompanying reliance index (RI) to evaluate its reliance level [11]. The RI is defined as the overlapping-area value between the standardized statistical distribution of the neural-network (NN) conjecture value and the multiple-regression (MR) predictive value [10], [11]. In other words, if a VMS possesses the RI scheme, then this VMS should have both the NN and MR VM results; while NN conjecture value is assigned as the default VM output and MR predictive value is considered as the reference output [10], [11]. However, as compared in [12] and [13], the MR algorithm may achieve superior accuracy with a stable process (such as low-level data variance), whereas the NN algorithm may have better accuracy when high-level data variance (e.g. process tool property drift or shift) occurs. To take advantage of the merits of both MR and NN algorithms, the simple-selection scheme (SS-scheme) was first proposed to enhance VM conjecture accuracy [14]. This SS-scheme simply selects either NN or MR output. Recently, to further improve the accuracy and with advanced studies, a weighted-selection scheme (WS-scheme), which computes the VM output with a weighted sum of NN and MR results, is presented.

One-hidden-layered back-propagation neural network (BPNN-I) is adopted as the algorithm for establishing the NN conjecture models. The CVD and photo processes in a fifth generation TFT-LCD factory are adopted as illustrated examples to test and compare the conjecture accuracy among solo-NN, solo-MR, SS-scheme, and WS-scheme. Test results show that the conjecture accuracy of the WS-scheme is the best among those solo-NN, solo-MR, SS-scheme, and WS-scheme algorithms.

The remainder of this paper is organized as follows. Section 2 details the SS-scheme and WS-scheme between NN and MR outputs. Section 3 then presents and compares the experimental results among solo-NN, solo-MR, SS-scheme and WS-scheme. The

The author would like to thank the National Science Council of R.O.C for financially supporting this research under contract Nos: NSC96-2622 -E-006-043 & NSC98-2622-E-006-009. This work was also supported by the Landmark Project of National Cheng Kung University, Taiwan.

Wei-Ming Wu, Fan-Tien Cheng (the corresponding author), Deng-Lin Zeng, and Jyun-Fang Chen are with the Institute of Manufacturing Engineering, National Cheng Kung University, Tainan 70101, Taiwan, R.O.C. (e-mail: min@super.ime.ncku.edu.tw; chengft@mail.ncku.edu.tw; delen@super.ime.ncku.edu.tw; yaya@super.ime.ncku.edu.tw), Tung-Ho Lin is with the Chung Shan Institute of Science and Technology, Taoyuan 32505, Taiwan, R.O.C. (e-mail: ldh6211@gmail.com), Min-Hsiung Hung is with the Department of Electrical and Electronic Engineering, National Defence University, Taoyuan 33509, Taiwan, R.O.C. (e-mail: mhhung@ndu.edu.tw).

implications of experimental results are also discussed here. Finally, a summary and conclusion are made in Section 4.

II. SS-SCHEME AND WS-SCHEME

Both the proposed SS-scheme and WS-scheme are all composed of an off-line classification flow of modeling data sets (as shown in Fig. 1). Then, the on-line selection flows of SS-scheme and WS-scheme are depicted in Figs. 2 and 3, respectively. They are described below.

2.1 Off-line Classification Flow of Modeling Data Sets

The entire modeling data sets are first classified into the NN group and the MR group based on the modeling error of each data set. The procedure shown in Fig. 1 is detailed as follows.

●Step 1) To create the NN and MR models, n sets of historical data are collected, including process data ($x_{a,j}$, a = 1, 2, …, n; j = 1, 2, …, p) from a production tool and the corresponding metrology data (y_a, a = 1, 2, …, n) from a metrology tool, where each set of process data contains individual parameters (from parameter 1 to parameter p). The correlation between the process and metrology data of each set should be assured before considering this set as a valid modeling set.

●Step 2) Before the NN conjecture model and MR predictive model are established, the process and metrology data have to be standardized by Z-score. The equations for standardizing the process and metrology data are listed as follows [11].

$$Z_{x_{a,j}} = \frac{x_{a,j} - \bar{x}_j}{\sigma_{x_j}}, \quad a = 1, 2, \ldots, n; \; j = 1, 2, \ldots, p \tag{1}$$

$$\bar{x}_j = \frac{1}{n}\left(x_{1,j} + x_{2,j} + \ldots + x_{n,j}\right) \tag{2}$$

$$\sigma_{x_j} = \sqrt{\frac{1}{n-1}\left[\left(x_{1,j} - \bar{x}_j\right)^2 + \left(x_{2,j} - \bar{x}_j\right)^2 + \ldots + \left(x_{n,j} - \bar{x}_j\right)^2\right]} \tag{3}$$

$$Z_{y_a} = \frac{y_a - \bar{y}}{\sigma_y} \tag{4}$$

$$\bar{y} = \frac{1}{n}\left(y_1 + y_2 + \cdots + y_n\right) \tag{5}$$

$$\sigma_y = \sqrt{\frac{1}{n-1}\left[\left(y_1 - \bar{y}\right)^2 + \left(y_2 - \bar{y}\right)^2 + \cdots + \left(y_n - \bar{y}\right)^2\right]} \tag{6}$$

where

$x_{a,j}$	jth process parameter in the ath set of process data;
$Z_{x_{a,j}}$	standardized jth process parameter in the ath set of process data;
$\bar{x}_j$	mean of the jth process data;
σ_{x_j}	standard deviation of the jth process data;
y_a	ath actual metrology value;
Z_{y_a}	standardized ath actual metrology value;
$\bar{y}$	mean of all the actual metrology values;
σ_y	standard deviation of all the actual metrology values.

●Step 3) The n sets of standardized process data ($Z_{x_{a,j}}$, a = 1, 2, …, n; j=1, 2, …, p) and the standardized actual metrology values (Z_{y_a}, a = 1, 2, …, n) are adopted to create the NN conjecture model and MR predictive model.

●Step 4) Compute the NN and MR modeling errors of each sample. The NN and MR modeling errors of each sample are depicted as follows.

$$\varepsilon_{N_a} = | y_a - \hat{y}_{N_a} |, \quad a = 1, 2, \ldots, n \tag{7}$$

$$\varepsilon_{r_a} = | y_a - \hat{y}_{r_a} |, \quad a = 1, 2, \ldots, n \tag{8}$$

where ε_{N_a} and ε_{r_a} represent the NN modeling error and MR modeling error for the ath sample, respectively; y_a is the actual metrology value; $\hat{y}_{N_a}$ and $\hat{y}_{r_a}$ are the NN and MR VM values, respectively.

●Step 5) Check whether ε_{N_a} is less than or equal to ε_{r_a} for each sample.

●Step 6) If ε_{N_a} is less than or equal to ε_{r_a}, then this modeling sample is distributed to the NN group. Otherwise,

this modeling sample is distributed to the MR group.

●Step 7) Assume that s and t sets of modeling sample data are contained in the NN group and MR group, respectively. Thus, the s and t sets of standardized model parameters are defined as $\boldsymbol{Z}_N = \left[Z_{N,1}, Z_{N,2}, \ldots, Z_{N,p}\right]^T$ (for NN group) and $\boldsymbol{Z}_r = \left[Z_{r,1}, Z_{r,2}, \ldots, Z_{r,p}\right]^T$ (for MR group). Here, $Z_{N,j}$ and $Z_{r,j}$ are the means of the standardized jth process parameters in the NN group and MR group, respectively.

2.2 On-line Selection Flow of the SS-scheme

Figure 2 shows the on-line selection flow between the NN and MR outputs for each conjecture sample (denoted the SS-scheme). The Mahalanobis distance (MD) between the conjecture sample and standardized model parameters of NN or MR group is first calculated. Then, the NN or MR output is chosen depending on which computed MD is smaller. The flow of the SS-scheme shown in Fig. 2 is detailed as follows.

●Step 1) Collect the newly (λth) input set of process data $\boldsymbol{X}_\lambda = \left[x_{\lambda,1}, x_{\lambda,2}, \ldots, x_{\lambda,p}\right]^T$ as the conjecture sample.

●Step 2) Compute the standardized λth set process data ($\boldsymbol{Z}_\lambda = \left[Z_{x_{\lambda,1}}, Z_{x_{\lambda,2}}, \ldots, Z_{x_{\lambda,p}}\right]^T$).

●Step 3) Calculate the Mahalanobis distance between $\boldsymbol{Z}_\lambda$ and $\boldsymbol{Z}_N$, and between $\boldsymbol{Z}_\lambda$ and $\boldsymbol{Z}_r$ as follows [11].

$$D^2_{N,\lambda} = \left(\boldsymbol{Z}_\lambda - \boldsymbol{Z}_N\right)^T \boldsymbol{R}_N^{-1} \left(\boldsymbol{Z}_\lambda - \boldsymbol{Z}_N\right) \tag{9}$$

$$D^2_{r,\lambda} = \left(\boldsymbol{Z}_\lambda - \boldsymbol{Z}_r\right)^T \boldsymbol{R}_r^{-1} \left(\boldsymbol{Z}_\lambda - \boldsymbol{Z}_r\right) \tag{10}$$

where $D^2_{N,\lambda}$ represents the MD between $\boldsymbol{Z}_\lambda$ and $\boldsymbol{Z}_N$, $D^2_{r,\lambda}$ depicts the MD between $\boldsymbol{Z}_\lambda$ and $\boldsymbol{Z}_r$, R_N^{-1} and R_r^{-1} are the inverse matrixes of correlation coefficients among the standardized parameters in the NN group and MR group.

●Step 4) Check whether $D^2_{N,\lambda}$ is less than or equal to $D^2_{r,\lambda}$.

●Step 5) If Step 4 is yes, then the NN output is selected, otherwise the MR output is chosen.

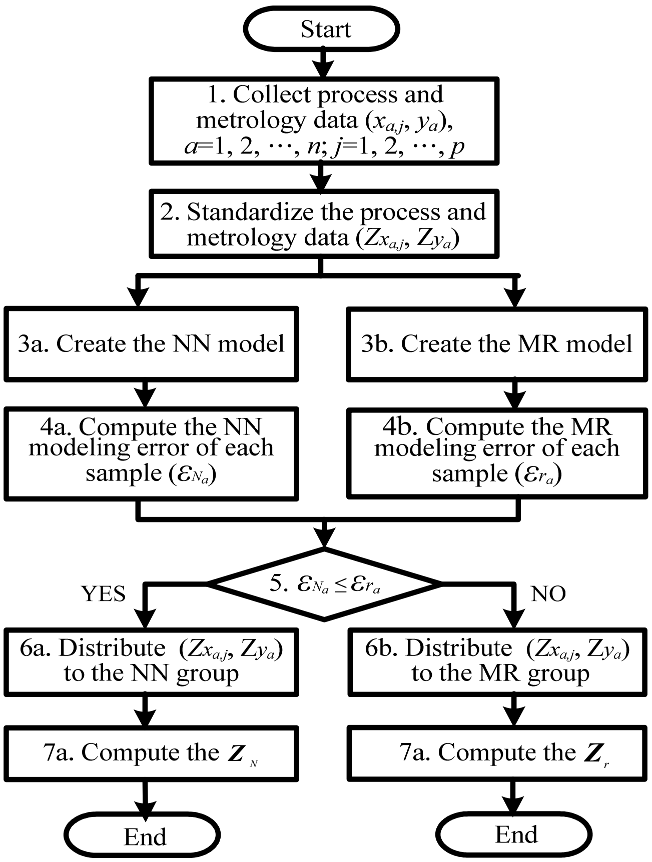

Fig. 1. Off-line Classification Flow of Modeling Data Sets

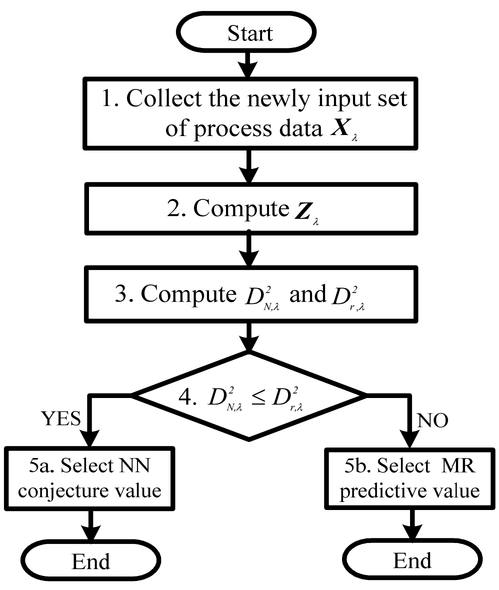

Fig. 2. On-line Selection Flow of the SS-scheme

2.3 On-line Selection and Computing Flow of the WS-Scheme

Figure 3 depicts the on-line selection flow with computing the weighted conjecture value for each conjecture sample (denoted the WS-scheme). The SS-scheme simply selects the VM conjecture output from either NN or MR result therefore the effect of accuracy-enhancement may be too extreme. To remedy this problem for further improving the VM conjecture accuracy, the WS-scheme is adopted by considering the weighted sum of NN and MR outputs. The selection and computing flow of the WS-scheme shown in Fig. 3 is detailed as follows.

●Steps 1) ~ 3) are the same as those of the SS-scheme.

●Step 4) Calculate the weighted conjecture value ($\hat{y}_{W_a}$) as follows.

$$\hat{y}_{W_a} = \frac{D^2_{N,\lambda}}{D^2_{N,\lambda}+D^2_{r,\lambda}}\hat{y}_{r_a} + \frac{D^2_{r,\lambda}}{D^2_{N,\lambda}+D^2_{r,\lambda}}\hat{y}_{N_a} \tag{11}$$

where $\hat{y}_{N_a}$ and $\hat{y}_{r_a}$ are the NN and MR VM outputs, respectively.

As shown in (11), the weighting of the NN component is determined by the ratio between $D^2_{r,\lambda}$ and the sum of $D^2_{N,\lambda}+D^2_{r,\lambda}$. On the contrary, the weighting of the MR component is calculated by the ratio between $D^2_{N,\lambda}$ and the sum of $D^2_{N,\lambda}+D^2_{r,\lambda}$.

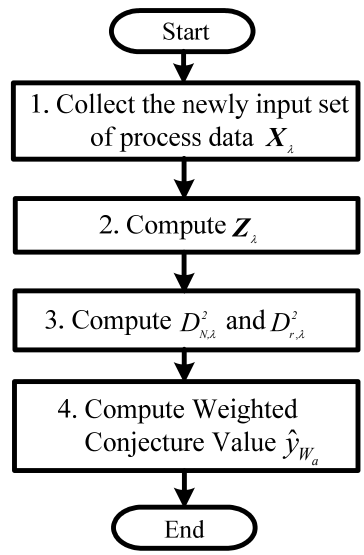

Fig. 3 On-line Selection and Computing Flow of the WS-Scheme

III. ILLUSTRATIVE EXAMPLES

Two examples are applied to be tested and compared. All the experimental data were collected from a CVD tool (for Example 1) and a photo tool (for Examples 2A and 2B). These CVD and photo tools are practically operating in a fifth generation TFT-LCD factory in Taiwan. In Example 1, to assure the quality of glass, 19 positions (shown in Fig. 4(a)) are measured on 19"-product glass for a single shoot CVD operation. In Examples 2A and 2B, 14.1"-product glass is divided into two shots for photo processing. Each shot has 8 measurement positions, as depicted in Fig. 4(b). Shot 2 is selected for Example 2.

Example 1 involves 92 sets of virtual cassettes and each virtual cassette may contain up to 100 pieces of glass. The last glass in a cassette is selected as the sample one, whose thickness value is measured to monitor the quality of the whole cassette. Thus, those process data ($\boldsymbol{X}_i$, i = 1, 2, …, 91) of the first 91 pieces of sampling glass and their corresponding actual metrology values (y_i, i = 1, 2, …, 91) are adopted for establishing the NN conjecture and MR predictive models.

The 92nd virtual cassette that contains 25 pieces of glass is used for the VM conjecturing test. For evaluating the conjecture accuracy, not only the regular sampling glass but the other 24 pieces of glass in the testing (92nd) cassette are measured. Therefore, the process data of these 25 pieces of glass in the testing cassette are used for VM conjecturing, whereas the corresponding actual metrology values of these 25 pieces of testing glass are adopted to evaluate the VM conjecture accuracy.

Example 2A includes 121 sets of process data and their corresponding metrology data. The first 102 sets are adopted as the modeling sets for establishing the NN conjecture and MR predictive models. The last 19 sets of process data are used for the VM conjecturing test, whereas the corresponding actual metrology values of those 19 sets are adopted for evaluating the VM conjecture accuracy.

Example 2B involves Example 2A's 121 sets and 12 additional sets of process and metrology data. Those 121 sets are adopted as the data for establishing the NN conjecture and MR predictive models. The additional 12 sets are applied for the VM conjecturing test. Especially, among those additional 12 sets, #3 ~ #9 are chosen to perform a critical dimension (CD) spread test with the adjustment of a major parameter on the photo equipment.

According to the physical properties of the CVD equipment and photo equipment, 10 and 21 key process parameters are chosen respectively as the inputs of the conjecture model. The conjecture accuracy calculated from the test data was quantified by the mean absolute percentage error (MAPE) [11], [15]. Its formula is represented as follows.

$$\text{MAPE} = \frac{\sum_{i=1}^{q} |(\hat{y}_i - y_i)/y|}{q} \times 100\% \qquad (12)$$

where $\hat{y}_i$ is the VM conjecture value, y_i is the actual metrology value, y is the target value, and q is the conjecture sample size. The closer the MAPE value is to zero, the better the conjecture accuracy of the model can achieve.

Besides the MAPE, this paper also proposes an accuracy index (AI), lying between 0 and 1, to make the accuracy evaluation more distinct. The AI formula of a test set for various algorithms is represented as follow. Each test set contains many samples.

$$\text{AI} = \frac{\text{MAPE}_{Algorithm} - \text{MAPE}_{Best}}{\text{MAPE}_{Worst} - \text{MAPE}_{Best}} \qquad (13)$$

where $\text{MAPE}_{Algorithm}$ represents the MAPE of solo-NN, solo-MR, SS-scheme, or WS-scheme algorithm of the test set; MAPE_{Best} is the MAPE value by selecting the smaller-error VM output of each NN-and-MR-output pair of all samples in the test set; and MAPE_{Worst} is the MAPE value by selecting the larger-error VM output of each NN-and-MR-output pair of all samples in the test set.

Observing (13), if $\text{MAPE}_{Algorithm}$ equals MAPE_{Best}, then AI equals 0. On the other hand, if $\text{MAPE}_{Algorithm}$ equals MAPE_{Worst}, then AI equals 1. The purpose of adding the selection schemes is to generate a smaller MAPE value of the test set. Therefore, the AI value is the smaller the better. However, the AI value may be smaller than 0 if the selection scheme generates a MAPE value that is smaller than MAPE_{Best}.

The detailed test results of the two examples mentioned above are presented below.

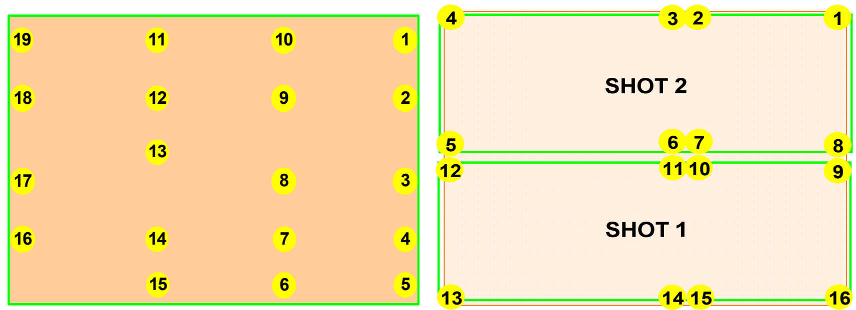

(a) (b)

Fig. 4 Measurement Positions of (a) CVD Equipment (19"-product Glass) (b) Photo Equipment (14.1"-product Glass).

3.1 Conjecture Results of Example 1

Among all the 19 measurement positions for the CVD process of 19"-product glass, the VM conjecture results of Positions 6 and 14 for various algorithms are illustrated in Fig. 5. The various AIs (0.57, 0.43, 0.41, and 0.35 for solo-NN, solo-MR, SS-scheme, and WS-scheme, respectively) shown in Fig. 5(a) indicate that the SS-scheme is better than the solo-NN and solo-MR as far as the VM conjecture accuracy is concerned. Moreover, the accuracy of the WS-scheme is superior to that of the SS-scheme. However, as shown in Fig. 5(b), the AIs of the solo-NN, solo-MR, and SS-scheme are all 0.50. This fact indicates that the SS-scheme cannot improve the accuracy of Position 14. Nevertheless, the accuracy is improved by applying the WS-scheme with AI = 0.42.

Table I presents the conjecture accuracy of the solo-NN, solo-MR, SS-scheme, and WS-scheme algorithms for all the (19) measurement positions of Example 1. As indicated in Table I, the accuracy of Positions 5, 13, and 14 of the solo-NN is better than that of the solo-MR. On the contrary, the solo-MR's accuracy of all the other positions is superior to the solo-NN's accuracy. That is one of the reasons why we try to develop the SS-scheme and WS-scheme to improve the overall accuracy. Observing the last row of Table 1, the means of MAPE and AI of the WS-scheme are the best among all the solo-NN, solo-MR, SS-scheme, and WS-scheme algorithms. And, the mean of AI of the SS-scheme is worse than that of the solo-MR in this example. Moreover, among those 19 positions, there are six positions (2, 4, 13, 15, 16, & 18) whose AI values of the SS-scheme are larger than 0.5 while only one position (11) whose AI value of the WS-scheme is larger than 0.5. Therefore, the WS-scheme is indeed better than the SS-scheme.

3.2 Conjecture Results of Example 2A

The glass of 14.1" product for the photo process has two shots. Each shot has 8 measurement positions. This example utilizes the eight positions of Shot 2, as shown in Fig. 4(b), for evaluation. Table II presents the VM conjecture accuracy of various algorithms for all the measurement positions (1-8). Among those 8 positions, the conjecture results of Positions 3 and 4 for various algorithms are depicted in Fig. 6. After examining Fig. 6 and Table II, we discover that the same conclusions made in Example 1 are still valid in Example 2A. The conclusions are accuracy improvement of the WS-scheme is assured because none of the AI values are greater than 0.5; and, that of the SS-scheme is not certain since the AI values of Positions 1, 2, 5, and 8 are greater than 0.5.

The experimental data of both Examples 1 and 2A are collected from normal CVD and photo manufacturing processes. To test the capability of the WS-scheme for improving the accuracy under process drift and/or shift conditions, Example 2B is presented as follows.

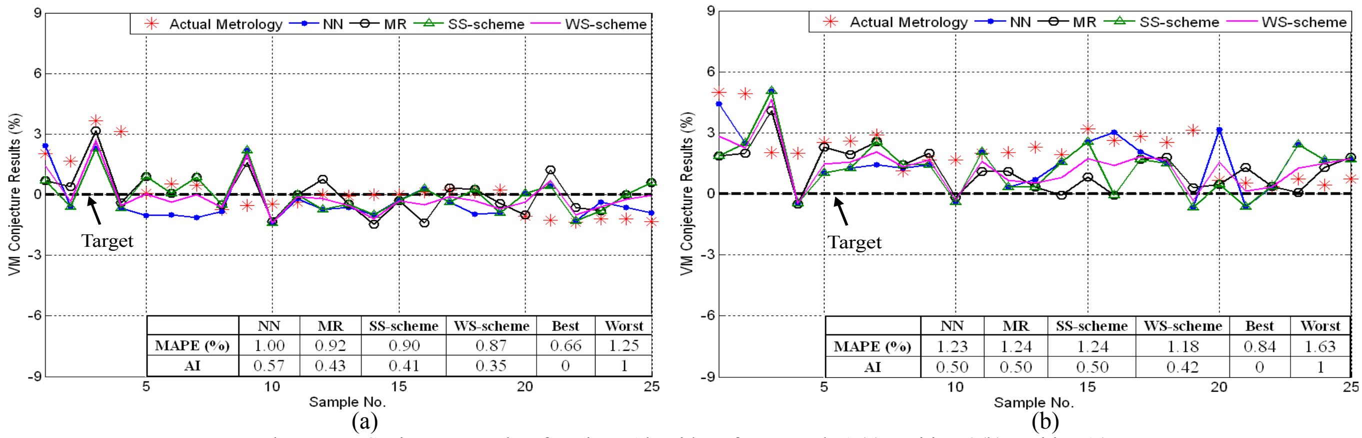

Fig. 5. VM Conjecture Results of Various Algorithms for Example 1 (a) Position 6 (b) Position 14.

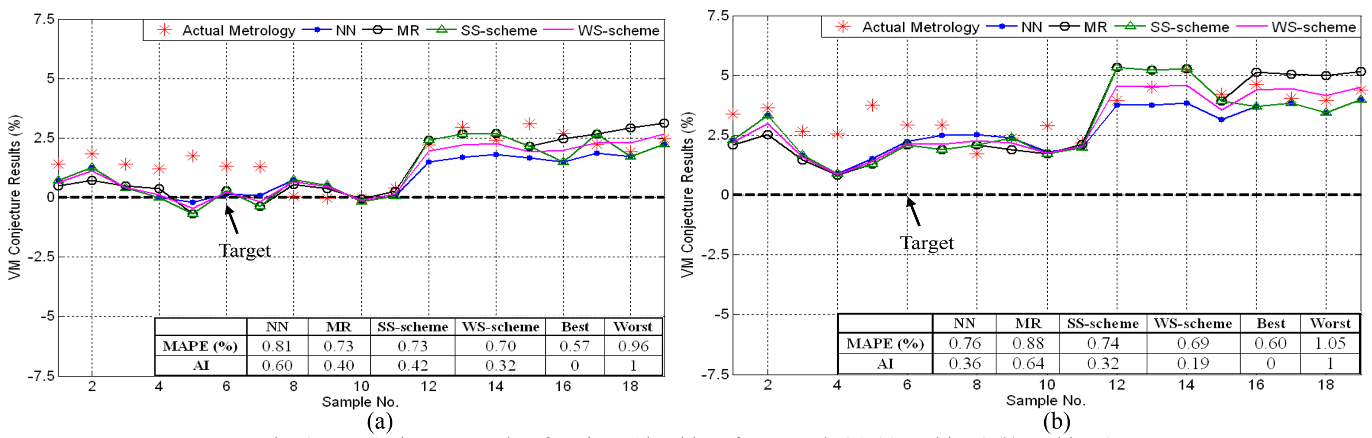

Fig. 6. VM Conjecture Results of Various Algorithms for Example 2A (a) Position 3 (b) Position 4.

TABLE I
VM CONJECTURE ACCURACY OF VARIOUS ALGORITHMS FOR EXAMPLE 1 (All Positions)

Pos.	Accuracy											
	MAPE (%)						AI					
	NN	MR	SS-scheme	WS-scheme	Best	Worst	NN	MR	SS-scheme	WS-scheme	Best	Worst
1	1.13	0.72	0.86	0.83	0.57	1.28	0.78	0.22	0.41	0.38	0	1
2	1.03	1.01	1.10	0.97	0.66	1.39	0.51	0.49	0.61	0.43	0	1
3	1.22	1.17	1.10	1.17	0.59	1.81	0.52	0.48	0.42	0.47	0	1
4	1.03	0.84	1.02	0.90	0.62	1.26	0.65	0.35	0.63	0.43	0	1
5	1.10	1.19	1.13	0.99	0.73	1.55	0.45	0.55	0.49	0.32	0	1
6	1.00	0.92	0.90	0.87	0.66	1.25	0.57	0.43	0.41	0.35	0	1
7	1.39	1.04	1.14	1.11	0.76	1.68	0.69	0.31	0.42	0.38	0	1
8	1.45	1.39	1.36	1.32	1.10	1.74	0.55	0.45	0.41	0.35	0	1
9	1.05	0.91	0.94	0.91	0.59	1.37	0.59	0.41	0.44	0.42	0	1
10	1.23	0.88	1.00	0.93	0.60	1.51	0.69	0.31	0.44	0.36	0	1
11	1.19	1.17	1.10	1.19	0.79	1.57	0.51	0.49	0.39	0.51	0	1
12	1.29	1.23	1.09	1.26	0.90	1.62	0.54	0.46	0.26	0.50	0	1
13	1.42	1.44	1.43	1.39	1.04	1.82	0.49	0.51	0.51	0.45	0	1
14	1.23	1.24	1.24	1.18	0.84	1.63	0.50	0.50	0.50	0.42	0	1
15	1.13	1.05	1.19	1.02	0.76	1.43	0.56	0.44	0.64	0.40	0	1
16	1.27	0.92	1.14	0.97	0.73	1.47	0.74	0.26	0.56	0.33	0	1
17	1.49	1.49	1.44	1.43	0.96	2.01	0.50	0.50	0.46	0.44	0	1
18	1.43	1.32	1.46	1.31	0.95	1.81	0.56	0.44	0.59	0.42	0	1
19	1.25	1.13	0.92	1.10	0.79	1.60	0.58	0.42	0.17	0.39	0	1
Mean	**1.23**	**1.11**	**1.13**	**1.10**	**0.77**	**1.58**	**0.57**	**0.42**	**0.44**	**0.41**	**0**	**1**

TABLE II
VM CONJECTURE ACCURACY OF VARIOUS ALGORITHMS FOR EXAMPLE 2A (All Positions)

Pos.	Accuracy											
	MAPE (%)						AI					
	NN	MR	SS-scheme	WS-scheme	Best	Worst	NN	MR	SS-scheme	WS-scheme	Best	Worst
1	0.84	0.72	0.79	0.76	0.62	0.94	0.69	0.31	0.54	0.44	0	1
2	0.90	0.67	0.82	0.79	0.60	0.98	0.80	0.20	0.58	0.50	0	1
3	0.81	0.73	0.73	0.70	0.57	0.96	0.60	0.40	0.42	0.32	0	1
4	0.76	0.88	0.74	0.69	0.60	1.05	0.36	0.64	0.32	0.19	0	1
5	0.78	0.66	0.74	0.71	0.59	0.86	0.72	0.28	0.55	0.44	0	1
6	1.32	1.34	1.31	1.31	0.99	1.66	0.48	0.52	0.47	0.47	0	1
7	0.85	1.08	0.92	0.92	0.73	1.19	0.24	0.76	0.39	0.40	0	1
8	0.90	0.93	0.95	0.85	0.64	1.20	0.47	0.53	0.55	0.37	0	1
Mean	**0.89**	**0.88**	**0.87**	**0.84**	**0.67**	**1.10**	**0.52**	**0.48**	**0.47**	**0.39**	**0**	**1**

3.3 *Conjecture Results of Example 2B*

As explained in the beginning of Section 3, among those 12 test sets, #3 ~ #9 were chosen to perform a critical dimension (CD) spread test with the adjustment of a major parameter on the photo equipment. Table III illustrates the VM conjecture results of various algorithms for Example 2B. In particular, the conjecture results of Positions 4 and 8 are depicted in Fig. 7(a) and 7(b), respectively. Observing Fig. 7 and Table III, again the conclusions drew in Examples 1 and 2A are still effective for Example 2B. Furthermore, the AI values of the WS-scheme at Positions 5 and 8 are negative, which means the MAPE of the VM conjecture results generated by the WS-scheme is smaller than the MAPE $_{Best}$.

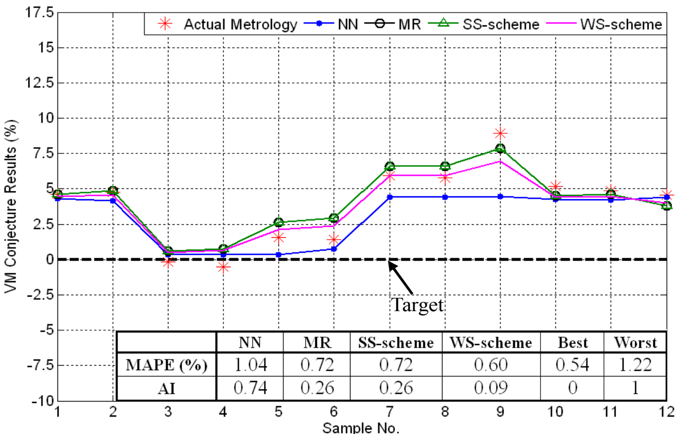

(a)

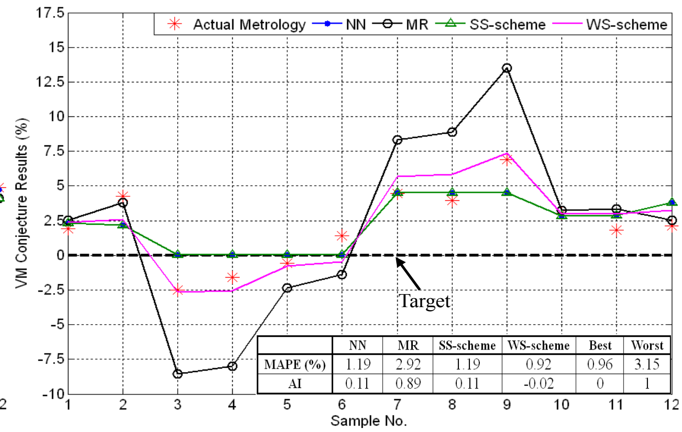

(b)

Fig. 7. VM Conjecture Results of Various Algorithms for Example 2B (a) Position 4 (b) Position 8.

TABLE III
VM CONJECTURE ACCURACY OF VARIOUS ALGORITHMS FOR EXAMPLE 2A (All Positions)

Pos.	Accuracy											
	MAPE (%)						AI					
	NN	MR	SS-scheme	WS-scheme	Best	Worst	NN	MR	SS-scheme	WS-scheme	Best	Worst
1	1.25	0.58	0.67	0.54	0.51	1.31	0.92	0.08	0.19	0.03	0	1
2	1.46	0.52	0.52	0.82	0.44	1.54	0.93	0.07	0.07	0.34	0	1
3	1.39	1.04	1.04	1.15	0.81	1.63	0.71	0.29	0.29	0.42	0	1
4	1.04	0.72	0.72	0.60	0.54	1.22	0.74	0.26	0.26	0.09	0	1
5	1.09	1.51	1.09	0.48	0.94	1.67	0.21	0.79	0.21	-0.63[a]	0	1
6	1.03	0.61	0.70	0.52	0.34	1.31	0.72	0.28	0.37	0.19	0	1
7	0.90	0.56	0.90	0.58	0.42	1.04	0.78	0.22	0.78	0.26	0	1
8	1.19	2.92	1.19	0.92	0.96	3.15	0.11	0.89	0.11	-0.02[a]	0	1
Mean	**1.17**	**1.06**	**0.85**	**0.70**	**0.62**	**1.61**	**0.56**	**0.44**	**0.24**	**0.08**	**0**	**1**

[a] Negative AI values indicate that the MAPE of the VM conjecture results is smaller than the MAPE $_{Best}$.

V. SUMMARY AND CONCLUSION

The SS-scheme that may choose the more accurate output between the dual NN and MR results for enhancing VM conjecture accuracy was proposed in CASE 2008. To further improve the accuracy, the WS-scheme, which computes the VM output with a weighted sum of NN and MR results, is developed in this paper. The CVD and photo processes of fifth generation TFT-LCD manufacturing are adopted as the illustrated examples to compare the VM conjecture accuracy among the solo-NN, solo-MR, SS-scheme, and WS-scheme algorithms. Test results show that the WS-scheme is the best among various algorithms for both CVD and photo processes and with normal as well as drift/shift manufacturing processes.

ACKNOWLEDGMENT

The authors would like to thank Chi Mei Optoelectronics Corporation, Ltd. (CMO) at Taiwan for providing the raw data of CVD and photo processes used in the illustrative examples.

REFERENCES

[1] J. Moyne, E. del Castillo, and A. M. Hurwitz, *Run-to-Run Control in Semiconductor Manufacturing.* Boca Raton, FL: CRC Press, 2001.

[2] A. Weber, “Virtual metrology and your technology watch list: ten things you should know about this emerging technology,” *Future Fab International*, issue 22, section 4, pp. 52-54, Jan. 2007.

[3] P.-H. Chen, S. Wu, J. Lin, F. Ko, H. Lo, J. Wang, C.-H. Yu, and M.-S. Liang, “Virtual metrology: a solution for wafer to wafer advanced process control,” in *Proc. 2005 IEEE International Symposium on Semiconductor Manufacturing (ISSM 2005)*, pp. 155-157, Sept. 2005.

[4] Y.-C. Chang and F.-T. Cheng, “Application development of virtual metrology in semiconductor industry,” in *Proc 31st Annual Conference IEEE Industrial Electronics,* Raleigh, NC, Nov. 2005, pp. 124-129.

[5] A. A. Khan, J. R. Moyne, and D. M. Tilbury, “An approach for factory-wide control utilizing virtual metrology,” *IEEE Transactions on Semiconductor Manufacturing*, vol. 20, no. 4, pp. 364-375, Nov. 2007.

[6] A. A. Khan, J. R. Moyne, and D. M. Tilbury, “Virtual metrology and feedback control for semiconductor manufacturing processes using recursive partial least squares,” *Journal of Process Control*, vol. 18, pp. 961-974, 2008.

[7] M.-F. Wu, C.-H. Lin, D. S.-H. Wong, S.-S. Jang, and S.-T. Tseng, “Performance Analysis of EWMA Controllers Subject to Metrology Delay,” *IEEE Transactions on Semiconductor Manufacturing*, vol. 21, no. 3, pp. 413-425, August 2008.

[8] F. Ko, C.-W. Lai, K. Zuo, H. Lo, J. Wang, P.-H Chen, C.-H Lin, and C.-H Yu, “Novel methodology to realize automatic virtual metrology,” United States Patent, Pub No.: US 2008/0275586 A1, Nov. 2008.

[9] T.-H. Lin, F.-T. Cheng, W.-M. Wu, Chi-An Kao, A.-J. Ye, and F.-C. Chang, "NN-based key-variable selection method for enhancing virtual metrology accuracy," *IEEE Transactions on Semiconductor Manufacturing*, vol. 22, no. 1, pp. 204-211, February 2009.

[10] F.-T. Cheng, H.-C. Huang, and C.-A. Kao, “Dual-phase virtual metrology scheme,” *IEEE Transactions on Semiconductor Manufacturing*, vol. 20, no. 4, pp. 566-571, Nov. 2007.

[11] F.-T. Cheng, Y.-T. Chen, Y.-C. Su, and D.-L. Zeng, "Evaluating reliance level of a virtual metrology system," *IEEE Transactions on Semiconductor Manufacturing*, vol. 21, no. 1, pp. 92-103, Feb. 2008.

[12] I. S. Markham and T. R. Rakes, “The effect of sample size and variability of data on the comparative performance of artificial neural networks and regression,” *Computers and Operations Research*, vol. 25, no. 4, pp. 251-263, 1998.

[13] Y.-C. Su, T.-H. Lin, F.-T. Cheng, and W.-M. Wu, "Accuracy and real-time considerations for implementing various virtual metrology algorithms," *Transactions on Semiconductor Manufacturing*, vol. 21, no. 3, pp. 426-334, Aug. 2008.

[14] W.-M. Wu, F.-T. Cheng, D.-L, Zeng, T.-H. Lin, J.-F. Chen, " Developing a selection scheme for dual virtual-metrology outputs," in *Proc. 2008 IEEE International Conference on Automation Science and Engineering,* Washington, D.C., U.S.A, Aug. 2008, pp.230-235.

[15] Y.-C. Su, M.-H. Hung, F.-T. Cheng, and Y.-T. Chen, “A processing quality prognostics scheme for plasma sputtering in TFT-LCD manufacturing,” *IEEE Transactions on Semiconductor Manufacturing*, vol. 19, no. 2, pp. 183-194, May 2006.